An HBT Excitation Function at the AGS

M.A. Lisa[j], for the E895 Collaboration
N.N. Ajitanand[m], J. Alexander[m], D. Best[a], P. Brady[e], T. Case[a], B. Caskey[e], D. Cebra[e], J. Chance[e], I. Chemakin[d], P. Chung[m], V. Cianciolo[i], B. Cole[d], K. Crowe[a], A.C. Das[j], J. Draper[e], S. Gushue[b], M. Gilkes[l], M. Heffner[e], H. Hiejima[d], A. Hirsch[l], E. Hjort[l], L. Huo[g], M. Justice[h], M. Kaplan[c], J. Klay[e], D. Keane[h], J. Kintner[f], D. Krofcheck[k], R. Lacey[m], J. Lauret[m], E. LeBras[m], H. Liu[h], Y. Liu[g], R. McGrath[m], Z. Milosevich[c], D. Olson[a], S. Panitkin[h], C. Pinkenburg[m], N. Porile[l], G. Rai[a], H.-G. Ritter[a], J. Romero[e], R. Scharenburg[l], L. Schroeder[a], R. Soltz[i], B. Srivastava[l], N.T.B. Stone[b], T.J. Symons[a], S. Wang[h], R. Wells[j], J. Whitfield[c], T. Wienold[a], R. Witt[h], L. Wood[e], X. Yang[d], W. Zhang[g], Y. Zhang[d]
[a]Lawrence Berkeley Lab, [b]Brookhaven National Lab, [c]Carnegie Mellon University, [d]Columbia University, [e]U.C. Davis, [f]St. Mary's College, [g]Harbin Institute, China, [h]Kent State University, [i]Lawrence Livermore National Lab, [j]The Ohio State University, [k]University of Auckland, NZ, [l]Purdue University, [m]SUNY at Stony Brook

The E895 Collaboration has measured Au+Au reactions at 2, 4, 6, and 8 AGeV with a very large acceptance Time Projection Chamber, at the Brookhaven AGS. Studies of reactions at these energies are sensitive to nuclear matter at the highest baryon density. It has been suggested that such conditions may trigger the transition to the Quark Gluon Plasma (QGP). Signatures of such a transition may include large lifetimes as measured by HBT techniques. Here, we present the first excitation function of pion inteferometry at intermediate AGS energies. Analyses of the correlation function in the Bertsch-Pratt and Yano-Koonin parametrizations provide insight into the π^--emitting source size, lifetime, and longitudinal flow. No large jumps in the HBT signals are observed as the beam energy is increased. Preliminary comparisons with RQMD calculations are given.

1 Introduction

1.1 E895 Motivation

A primary goal of high-energy heavy ion physics is to create and study the quark-gluon plasma (QGP), a phase of matter in which partonic– instead of hadronic– degrees of freedom describe the system. Transport, hydrodynamic, and nucleation theories [1,2,3,4] suggest that energy densities achieved in central heavy ion collisions at AGS energies may be sufficient to create the QGP.

If the QGP is created in a heavy ion collision, the timescale for particle emission is expected to be longer than a scenario in which only ordinary hadronic degrees of freedom play a role [5,6], due to the extra time of hadronization. Thus, one proposed signature for QGP formation has been a large apparent source lifetime as measured by pion HBT measurements. However, HBT analyses of very heavy ion collisions at the maximum AGS energy [7,8]

(10.6 AGeV) and at CERN SPS [9,10] (158 AGeV) do not indicate emission timescales longer than about 4 fm/c, which is consistent with the time distribution from normal hadronic physics models. Thus, it may seem pointless to look for long lifetimes at energies *below* maximum AGS energy.

However, recent hydrodynamical calculations by Rischke and collaborators [6] suggest that some signatures of QGP creation– including flow and large source lifetimes from HBT– may best be studied with excitations functions, which would scan the energy density of the system through the QGP threshold energy, or "softest point" in the Equation of State [6,11,12]. For a source created at this energy, the lifetime is longer because the system does not expand and cool as rapidly as it would if there were no phase transition. For collisions at energies very much above this threshold energy, the system (which is in the QGP phase) expands and cools rapidly, and the lifetime effect is diminished.

Finally, any excitation function study serves as a stringent test of transport models, which represent our understanding of the dynamics of heavy ion collisions. As these models prepare to deal with data from ever higher bombarding energies, we would do well to constrain– and understand the relative importance of– physical assumptions in them, such as effects due to the nuclear meanfield.

1.2 Measurement and Experimental Issues for HBT

Using the Time Projection Chamber [13,14] used in the EOS experiments at the Bevalac, the E895 collaboration has measured about 0.5-1 million collisions at 2, 4, 6, and 8 AGeV at the Brookhaven AGS. The results presented here represent roughly 50% (25%) of the total statistics at 4 and 8 (2 and 6) AGeV.

The TPC was located in the MPS magnet operated with a field of 0.75 or 1 T. The active volume of the TPC is a rectangular region 154 cm x 96 cm x 75 cm in the beam, bend, and drift directions, respectively. Electrons liberated by charged particles passing through the TPC drift to 15360 pads arranged in 128 rows at the bottom of the TPC. The signal on each pad is sampled and digitized every 100 ns (140 time buckets), providing about 2 million 3-dimensional pixels in which the ionization is measured. "Hits" are reconstructed from the pixels, corresponding to a track crossing a padrow. Tracks are formed from the hits, giving continuous tracking with nearly 4π acceptance in the c.m.

Event reconstruction results are processed by the HBT analysis after passing a series of quality cuts. The most important for this analysis are an event-wise primary vertex cut, to ensure that the interaction comes from the target, and a track-wise cut requiring that the track project back to the primary interaction; this latter removes many π^- from weak decays (e.g. Λs) as well as ghost tracks from unused hit combinatorics.

Particle identification in the TPC is performed by correlating the magnetic rigidity of a track with its specific ionization in the gas. In this space, the electron band overlaps somewhat the π^- band; with cuts, we estimate the level of e^- contamination at about 5%. We find that relaxing the PID cuts to purposely allow more electrons into our π^- sample affects only the HBT λ, not the radii. Negative kaon contamination is insignificant at these energies.

The momentum resolution from the tracking software itself is about 1%, but more important is the contribution from multiple coulomb scattering in the target (a 3% interaction target was used), which worsens the overall resolution to 1.5-3%. The resolution in terms of relative momentum is as poor as 12 MeV/c in 8 AGeV reactions. Prescriptions exist for correcting the correlation signal for resolution effects (e.g. that developed by the NA44 collaboration [15]). While we have attempted such corrections previously with some success[16], subtle imperfections in the E895 simulator made our implementation unstable. In the present analysis, we do not correct the data for resolution, but instead smear the RQMD predictions by our resolution in order to compare correlation functions directly.

Tracks which are very close in the TPC can merge and appear as a single track, leading to a large suppression in the correlation function at low relative momentum. To correct for this, we require (in both the numerator and denominator of the correlation function) that the two tracks have well-seperated hit positions on at least 15 padrows. (In applying this cut to the mixed events, we account for event-to-event differences in primary vertex position.) Further increasing the required hit seperation distance or number of padrows does not affect the measured correlations. Simulations show that this also obviates the need for a further track-splitting cut; false "pairs" from split tracks are eliminated by this cut.

1.3 Coulomb correction

Throughout this work, the Coulomb correction applied to the correlation functions is obtained by averaging the square of the Coulomb wave function [17,18] over a spherical Gaussian source of 5 fm radius. This radius is consistent with those extracted from 3-dimensional fits to the correlation function (see below); changing the radius used in the Coulomb correction by ± 1 fm has negligible effect on the fit parameters. Our correction is the same as used by the E877 collaboration [7], and equivalent to that used by NA49 [10]. Identical Coulomb corrections are applied to the data and to RQMD model predictions.

2 1-D Correlation Functions at Midrapidity

For a first analysis of the correlation function, we concentrate on π^- emitted at midrapidity ($y = y_{c.m.} \pm 0.25$) from central collisions ($\sim 10\%\sigma_T$). In order to compare our results with those of E866/917 [8,19], we require p_T¿100 MeV/c.

The quality of the data is apparent in Figure 1, which shows correlation functions at the four bombarding energies, as a function of $Q_{inv} \equiv (\vec{Q}^2 - (Q^0)^2)^{1/2}$. While interpretation of the parameters from a Gaussian fit to the 1-dimensional correlation function is not straightforward, and the χ^2 values for the lower energies are significantly larger than unity (see Fig. 1), the bombarding energy systematics of the parameters can be investigated and the values compared to those extracted by others. Therefore, also shown are fits to the conventional Gaussian form $C(Q_{inv}) = 1 + \lambda e^{-Q_{inv}^2 R_{inv}^2}$, where the lowest Q-bin is excluded from the fit). The bombarding energy dependence of the R_{inv} and λ is shown in Figure 2. The data show no obvious jumps flagging a phase transition, and lead smoothly to the result of E866 [8].

Also shown for the energies measured by E895 are the results of fits to the correlation function using the RQMD model [20] (v2.3) and the correlator code (CRAB) of Pratt [21]. Sets of events with b=0-5 fm, geometrically weighted, were generated with RQMD run in the cascade mode, and also with the mean field on. As compared to the results for the cascade events, the calculations with the mean field show a stronger E_{beam} dependence of the fit parameters, and, especially for λ, appear to reproduce the data a bit better.

The fitted 1-D radius parameter appears relatively constant at roughly 5.5 fm for $E_{beam} = 4-11$ AGeV, but is considerably larger at 2 AGeV (however we note again that the χ^2 value is larger as well). This trait is not predicted by the RQMD model. Further analysis of the 2 AGeV data with more statistics will be required to confirm this possible increase at low energy, but it is interesting to note that the radius extracted (through somewhat different analysis) by the FOPI collaboration for Au+Au collisions at 1.06 AGeV is similarly large ($R_{inv} \approx$7.5 fm) [23].

3 Excitation Function of Multi-dimensional HBT

To explore the correlations in more detail, we have performed multi-dimensional fits to the correlations. In the system center of mass frame, we decomposed the relative momentum vector in the Bertsch-Pratt parametrization [22], and fit the 3-dimensional correlation function with

$$C(q_{out}, q_{side}, q_{long}) = 1 + \lambda e^{(-R_{out}^2 q_{out}^2 - R_{side}^2 q_{side}^2 - R_{long}^2 q_{long}^2 - 2R_{ol}^2 q_{out} q_{long})} \quad (1)$$

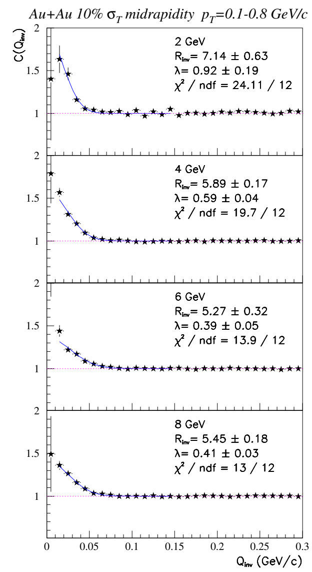

Figure 1: Correlation functions in Q_{inv} for midrapidity π^- with p_T >0.1 GeV/c from central collisions at the four bombarding energies measured. Data is shown by stars, while Gaussian fits are indicated by the lines.

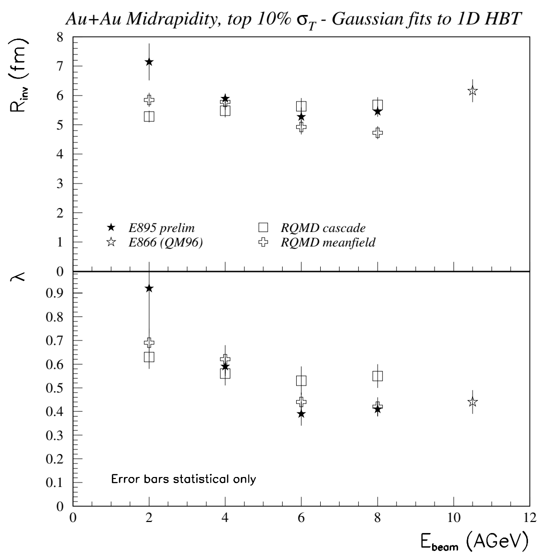

Figure 2: The excitation function of Gaussian fit parameters for 1-dimensional correlation functions measured at midrapidity by E895 (filled stars) and E866[8] (empty star). Also shown are results to fits of correlations obtained from the output of the RQMD model with (crosses) and without (squares) the meanfield. Note that the E895 data is not corrected for momentum resolution, and the RQMD calculations have been smeared by the E895 resolution.

The particles were ordered such that $q_{long} > 0$. Figure 3 shows projections of the correlation functions and the fits for correlations measured at midrapidity and $p_T = 0.1 - 0.8$ GeV/c from central collisions. The projections in a given component are integrated over the other two components in the range ± 30 MeV/c, and the curves in the figure are projections of the fits weighted by number of event-mixed pairs in each bin. Statistics were insufficient to perform the multidimensional analysis for the 2 AGeV dataset and required a relaxed rapidity window for the 6 AGeV set.

The cross-term [24] R_{ol}^2 (which may be negative) was included in all fits, but consistently comes out with very large uncertainty. At midrapidity and for low p_T, this term is expected to vanish. Fixing $R_{ol} = 0$ typically reduces the other radii by an amount which is within their uncertainties. Figure 4 shows the evolution of the 3-d fit parameters with bombarding energy, along

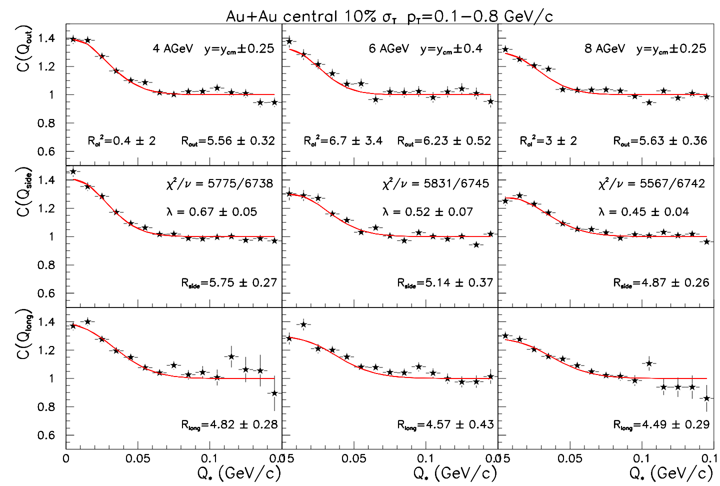

Figure 3: Projections of the measured correlation function decomposed in the Bertsch-Pratt convention for pions measured near mid-rapidity from central collisions at 4, 6, and 8 AGeV bombarding energy (columns left to right). Curves are projections of 3-dimensional fits. Projections in a q-component for both the data and the fits are integrated over the range $\pm 30 MeV/c$ in the two other components.

with the results of fits for RQMD events. The effect of momentum resolution (Section 1.2) on the correlation functions from RQMD is a reduction of $\sim 15\%$ in the extracted radii and 0.25 in λ.

Overall, the RQMD model reproduces the data fairly well, with or without meanfield effects. Some sensitivity to the meanfield may be present in the R_{long} parameter, which is smaller at the lower energies (and in better agreement with the data) when the meanfield is on. This may be due to enhanced sidewards expansion as compared to longitudinal flow, when the meanfield acts, which would dilute the system earlier and lead to smaller freezeout extension along the beam axis [25]; this possibility requires further study with the RQMD.

For almost all phasespace cuts studied at all beam energies, $R_{out} > R_{side} > R_{long}$, although this first inequality is violated for the 4 AGeV midrapidity cut shown. The decreasing difference between R_{side} and R_{long} observed in our data appears consistent with an evolutionanly trend with increasing energy; at the maximum AGS energy $R_{side} \approx R_{long}$ [7], and for SPS energies $R_{side} < R_{long}$ [9].

The decrease in λ is understood by enhanced production of long-lived resonances at higher energy. Although many π^- from decays of, e.g. Λ's, may be eliminated from the HBT analysis with a cut on the decay vertex, detailed

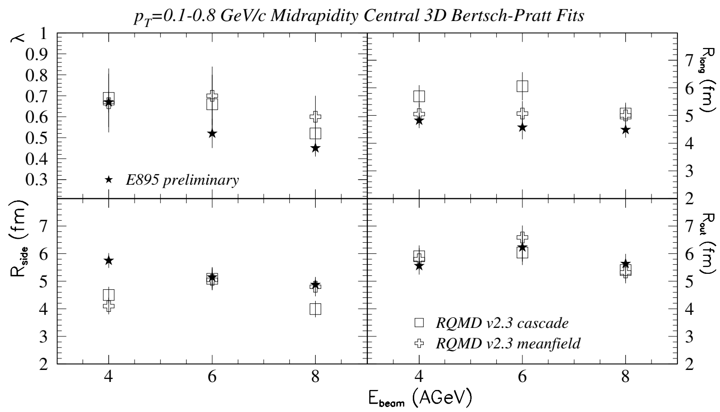

Figure 4: Bertsch-Pratt fit parameters to the 3-d correlations as a function of bombarding energy. Open symbols are the results of fits to RQMD-generated correlations.

simulations indicate that 5-10% of the π^- that pass our cuts come from weak decays. Especially at the lower energies, resonance production in the RQMD is suppressed when the meanfield is on; however this effect is not large enough to make a substantial difference to the correlation fits.

4 Multi-dimensional HBT at low p_T for 4 AGeV Central Collisions

A more detailed probe of the collision may come from studying the correlation function for small slices in phasespace. Here, we discuss only the 4 AGeV data at very low p_T (0-0.15 GeV/c) in narrow slices of rapidity; these correlations are not affected by the strong $\vec{x}-\vec{p}$ correlations in the transverse direction, and are likely to probe the longest-lived source.

Bertsch-Pratt (BP) fit parameters are shown in the left panel of Figure 5, for data and the two RQMD event sets, as a function of rapidity. At all rapidities, $R_{out} > R_{side}$, suggesting π^- emission over a finite timescale. To better characterize the timescale, we have also decomposed and fit the correlation function using the Yano-Koonin-Podgoretskiĭ (YK) parameterization [27]. There are several advantages to this parameterization: 1) the numerical values of the fit parameters are frame-independent, 2) the timescale R_0 is fit directly as opposed to being related to the difference of two large numbers $R_{out}^2 - R_{side}^2$, and 3) the velocity (rapidity) of the emitting source is also directly fit, thus providing direct information on the dynamical nature of the source.

On the right panels of Figure 5 are shown the YK timescale parameter R_0, the longitudinal radius $R_{||}$, and the source rapidity, as a function of y_{π^-}. The fits indicate an emission timescale on the order of 6.5 fm/c, in good agreement

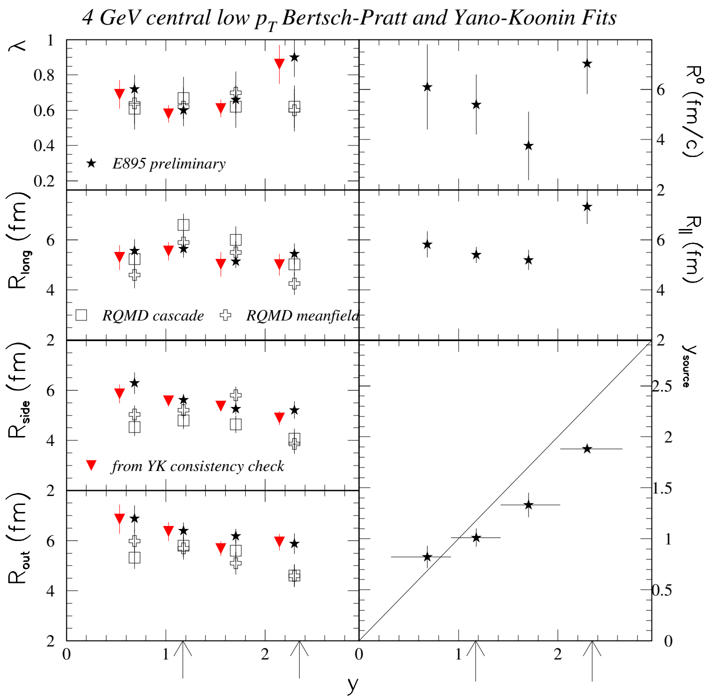

Figure 5: Bertsch-Pratt (left) and Yano-Koonin (right) fit parameters to measured π^- correlation functions for $p_T = 0 - 0.15$ GeV/c, as a function of lab rapidity. Bertsch-Pratt fits to RQMD-generated correlations are also shown. *Derived* Bertsch-Pratt parameters from the Yano-Koonin consistency relations are shown by inverted triangles, and are offset in rapidity for clarity; see text for details. Arrows indicate the beam and c.m. rapidity.

with the π^- time spectrum coming directly from RQMD, which has a Gaussian width of 7.5 fm/c. The longitudinal radius (in the local source frame) shows a large rise at beam rapidity, suggesting that π^- found at y_{beam} come from the middle of the fireball as well as the forward regions. This qualitative picture is also consistent with the lower right-hand panel, which plots the source rapidity as a function of y_{π^-}. A source characterized by boost-invariant longitudinal flow would show $y_{source} = y_{\pi^-}$ (solid line in figure), as is seen at SPS energies [28]. A static source (no longitudinal flow) would show a horizontal line $y_{source} = y_{c.m.}$, while the measured correlations at 4 AGeV correlations show evidence of non-boost invariant longitudinal flow.

It is clear that the correlation function contains the same information in both the YK or BP momentum decompositions, and a set of consistency relations has been worked out by Heinz [27], that relate the sets of parameters. In order to check for consistency of the analysis and stability in the fits, we have used these relations to derive the *expected* BP parameters from our measured YK parameters. The results are shown by the inverted triangles in the figure. (We note that the consistency relations give $R_{side}^{expected} = R_{\perp}$, so there is no need to plot the YK parameter $R_{\perp}$ seperately.) Within uncertainties, we see good consistency between the two (independent) decompositions.

Finally, also shown in Figure 5 are BP fit results to correlation functions from the RQMD. R_{side} and R_{out} are generally underpredicted at 4 AGeV for all rapidity. An identical analysis at 8 AGeV (not shown) shows that these parameters are well reproduced, with or without the meanfield on. As seen in Figure 4, R_{long} is better reproduced by RQMD with meanfield on at midrapidity, but the model shows a decrease in R_{long} away from $y_{c.m.}$ (similar to that seen at SPS energies), which is not observed in the data; data and model correlations disagree in a similar way at 8 AGeV.

5 Summary

In summary, we have presented the first intensity interferometry excitation function at AGS energies. For central collisions, no sharp jump in HBT fit parameters is seen as the bombarding energy is increased. Due to both increased resonance production and resolution effects, the intercept parameter λ falls with energy, in agreement with RQMD predictions. The ordering $R_{out} \gtrsim R_{side} > R_{long}$ likely indicates a source of finite lifetime (i.e. duration of emission). The relative size of R_{side} and R_{long} seems to evolve from a small R_{long} below maximum AGS energy to a large R_{long} at SPS. This may be due to the increased longitudinal motion coupled to a finite "relaxation time" before which particles are emitted.

Yano-Koonin fit parameters are seen to be consistent with the BP parameters. The source of very low p_T π^- from central collisions at 4 AGeV shows strong, but not boost-invariant, longitudinal flow, and an emission timescale of about 6 fm/c, in qualitative agreement with RQMD predictions.

Althought discrepancies between the data and model predictions exist and must be investigated, it appears that "standard" hadronic physics, as represented by RQMD, describes the π^- correlations well. Possible sensitivity in R_{long} to meanfield effects in the model will be investigated with more statistics.

Acknowledgments

This work supported by the U.S. Department of Energy under contract DE-AC03-76SF00098 and grants DE-FG02-89ER40531, DE-FG02-88ER40408, DE-FG02-87ER40324, by the U.S. National Science Foundation under grants PHY-

9722653, PHY-9601271, PHY-9225096, and by the University of Auckland Research Committee, NZ/USA Cooperative Science Programme CSP 95/33.

References

1. B.A. Li and C.M. Ko, Nucl. Phys. **A601**, 457 (1996).
2. J.I. Kapusta, A.P. Vischer, R. Venugopalan, Phys. Rev. C**51**, 901 (1995).
3. D. Rischke *et al.*, J. Phys. G14, 191, (1988); Phys. Rev. D**41**, 111 (1990)
4. N.K. Glendenning, Nucl. Phys. **A512**, 737 (1990).
5. S. Pratt, Phys. Rev. **C49** 2772 (1994); Phys. Rev. **D33**, 1314 (1986).
6. D.H. Rischke, nucl-th/96039; Nucl. Phys. **A610**, 88c (1996).
7. J. Barrette, *et al.* (E877), Nucl. Phys **A610**, 227c (1996); J. Barrette, *et al.*, Phys. Rev. Lett **78**, 2916 (1997).
8. M.D. Baker, *et al.* (E802), Nucl. Phys. **A610**, 213c (1996); B.A. Cole, *et al.* (E802), Nucl. Phys. **A590**, 179c (1995)
9. I.G. Bearden, *et al.* (NA44), Nucl. Phys. **A610**, 240c (1996)
10. K. Kadija, *et al.* (NA49), Nucl. Phys. **A610**, 248c (1996).
11. C.M. Hung and E.V. Shuryak, Phys. Rev. Lett. **75**, 4003 (1995).
12. D.H. Rischke, S. Bernard, J.A. Maruhn, Nucl. Phys. **A595**, 346 (1995).
13. H.G. Pugh, G. Odyniec, G. Rai, and P. Seidl, report LBL-22314 (1986).
14. G. Rai, *et al.*, IEEE Trans. Nucl. Sci. **37**, 56 (1990).
15. H. Bøggild, *et al.* (NA44), Phys. Lett. **B302**, 510, (1993); D. Hardtke, Ph.D. dissertation, The Ohio State University (1997).
16. M.A. Lisa *et al.* (E895), in Proceedings of Winter Workshop, Snowbird 1998. Plenum Press (in press).
17. S. Pratt, T. Csörgő, and J. Zimányi, Phys. Rev. **C42**, 2646 (1990); S. Pratt, Phys. Rev. **D33**, 72 (1986).
18. A. Messiah, **Quantum Mechanics**, North-Holland Publishing (1961).
19. J.H. Lee, contribution to these proceedings.
20. H. Sorge, Phys. Rev. **C52**, 3291 (1995).
21. S. Pratt, Quark Matter '93, *Nucl. Phys.* A **566**, 103c (1993)
22. G. Bertsch, M. Gong, and M. Tohyama, Phys. Rev. **C37** 1896 (1988); S. Pratt, Phys. Rev. **D33**, 1213 (1986).
23. D. Pelte, *et al.* (FOPI), Proceedings of the International Research Workshop, Poiana Brasov, Romania, World Scientific (1997), and contribution to these proceedings.
24. S. Chapman, P. Scotto, and U. Heinz, Phys. Rev. Lett. **22**, 4400 (1995).
25. H. Sorge, private communication.
26. S. Chapman, J.R. Nix, and U. Heinz, Phys. Rev. **C52**, 2694 (1995).
27. U. Heinz, Nucl. Phys. **A610**, 264c (1996).
28. R. Ganz, contribution to these proceesings.